TECHNICAL SIMULATIONS AND MEASUREMENTS OF CAGE-SWITCHING AT THE INDUCTION MACHINE

Tulbure Adrian*, Risteiu Mircea**

** University of Petrosani*
*** University „1 Decembrie 1918" Alba-Iulia*

Abstract: In the present paper the drive system with double-cage induction machine using differential equations will be mathematically modelled and simulated. The mathematical models represent the waveforms of electromagnetic quantities associated with the stator and rotor circuits as well as coresponding mechanical quantities. For examing the characteristic performance of the induction machine by switching between cages, the simulator softwares MATLAB and NETASIM have been used. The simulated current- and torque-waveforms will be compared with the experimental values. To practical validation of the results a mains operated induction machine with workingcage controller have been designed and tested in the Institute of Electrical Power Engineering in Clausthal, Germany.

Keywords: induction machine, drive sistem, cage switching, mathematical model, measurements, waveform.

1. SIMULATION AND VALIDATION OF THE SINGLE CAGE INDUCTION MACHINE

As an electrical part, the Induction Machine (IM) with direct connection to the power network (Fig.1) possesses damper and spring properties. The motor attenuation and the motor spring characteristics depend on the excitation frequency ω_A , speed of rotating field ω_d, breakdown slip s_K and breakdown torque respectively M_K (Beck et al., 2001), (Tulbure, 2003). The mechanical part (Fig.1) is assumed to be, with certain simplifications, a mathematical model of a two-mass-oscillator. This is characterised by the following mechanical parameters: masses with inertia (J_1,J_2), damping *(b),* spring stiffness *(c)* and the natural (self) frequency *(fe)* (Richter, 1983).

The mathematical model of the drive system with the mains-operated IM (Fig.1) can be described analytically after linearization by the following equations:

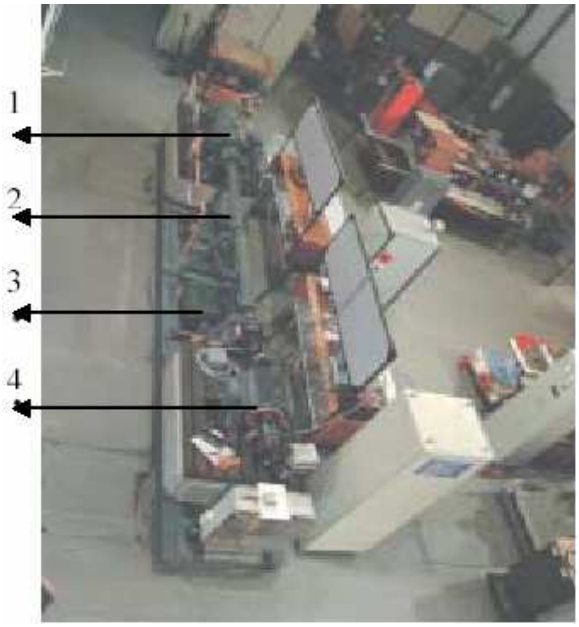

Fig.1 Structure of the drive system. 1. load as DC-motor, 2. flexible shaft, 3. one-cage induction machine, 4. double-cage induction machine

$$\Delta M_M = -(b_M \cdot p + c_M) \cdot \Delta\alpha_1 \qquad (1)$$

$$\Delta M_M = J_1 \cdot p^2 \cdot \Delta\alpha_1 + \Delta M_W \qquad (2)$$

$$\Delta M_W = b \cdot p \cdot (\Delta\alpha_1 - \Delta\alpha_2) + c \cdot (\Delta\alpha_1 - \Delta\alpha_2) \qquad (3)$$

$$\Delta M_W = J_2 \cdot p^2 \cdot \Delta\alpha_2 + \Delta M_L \qquad (4)$$

$$\omega_i = \frac{\mathrm{d}\alpha_i}{\mathrm{d}t} \qquad p = \frac{\mathrm{d}}{\mathrm{d}t} \qquad (5)$$

where:

J_1	motor inertia;	J_2	load inertia
M_M	motor torque;	M_W	shaft torque
ML	load torque	p	Laplace operator
b	attenuation coefficient of the shaft		
c	spring coefficient of the shaft		
b_M	attenuation coefficient of the motor		
c_M	spring coefficient of the motor		
ωi	rotation speed of the system		
$\alpha 1$, $\alpha 2$	mechanical angle of the motor respectively load.		

$$v = \frac{\omega_A}{s_k \cdot \omega_d} \qquad \text{specific excitation frequency}$$

$$\lambda = \frac{s}{s_k} \qquad \text{average slip}$$

The motor coefficients c_M and b_M depend on the excitation frequency ω_A, speed of rotating field ω_d., breakdown slip and torque s_K respectively M_K (Richter, 1983), (Beck et al. 2001) and can be calculated as follows:

$$b_M = \frac{2 \cdot (1 + v^2 - \lambda^2)}{s_K \cdot \left[(1 + \lambda^2 - v^2) + 4 \cdot v^2\right]} \cdot M_K \qquad (6)$$

$$c_M = \frac{2 \cdot v^2 (1 + v^2 - 3 \cdot \lambda^2)}{(1 + \lambda^2) \cdot \left[(1 + \lambda^2 - v^2) + 4 \cdot v^2\right]} \cdot M_K \qquad (7)$$

1.1. Simulation in the frequency domain

From the relations presented above, the different transfer functions for the electromechanical system can be calculated. In order to analyse the dynamic behaviour of the IM in frequency domain, the Bodediagram for the signal path $\Delta M_W \rightarrow \Delta M_L$ has been simulated with the help of the MATLAB-software.

The transfer function F(p) shaft-torque / load-torque fluctuation is described by the following equation (8).

$$F(p) = \frac{(J_1 p^2 + b_M p + c_M) \cdot (bp + c)}{\left[J_1 p^2 + (b_M + b) p + c_M\right](J_1 p^2 + bp + c) - (bp + c)^2}$$

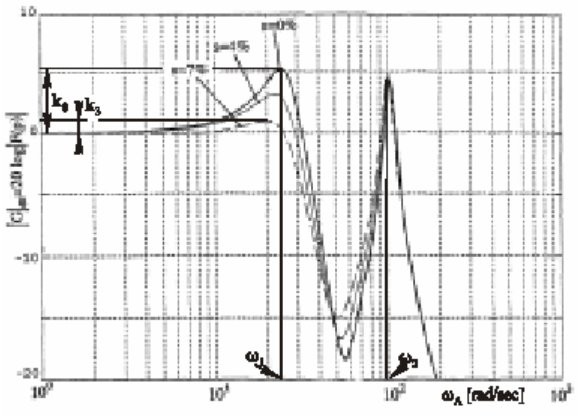

Fig.2 Bode-diagram of the transfer function $F(p) = \Delta M_W(p) / \Delta M_L(p)$ in correlation with excitation frequency ω_A,and the slip value *s*.

The transfer function (8) will have the following final form (polinomial function of 7 order):

$$F(p) = \frac{a_7 p^7 + a_6 p^6 + \ldots + a_1 p + a_0}{b_8 p^8 + b_7 p^7 + \ldots + b_1 p + b_0} \qquad (9)$$

From this, the oscillation magnitude will be obtained:

$$\left|F(\mathrm{j}\omega_A\right|_{dB} = 20 \log\left|\mathrm{Re}\{F\} + \mathrm{j}\,\mathrm{Im}\{F\}\right| \qquad (10)$$

Figure 2 shows the frequency response characteristic for the transfer function *F(p) (Matlab, 2005*) as a function of the stationary operating point (slip) of the machine. In this diagram a scaling up to the factors k_0 =5 dB (at no-load operation, s=0%) respectively k_3=1dB (at the load operation mode with s=7%) is to be observed.

1.2. Simulation in the time domain

The whole electromechanichal system has been modelled using a new programmed macro-bloc of the simulation program (Netasim, 1992). The dynamic model of the induction motor is described within a system of coordinates with two rectangular axes α and β. The generated torque (11) can be expressed in terms of rotor currents and rotor flux linkages (Schröder, 2001). The load torque will be represented (12) through the Load Input Function:

$$M_M = \frac{3}{2} \cdot Z_p \cdot (\Psi_{2\beta} \cdot i_{2\alpha} + \Psi_{2\alpha} \cdot i_{2\beta}) \qquad (11)$$

$$M_L = M_0 + \Delta M_{L0} \cdot \sin \Omega_A t \qquad (12)$$

where:

M_0 = basic load torque

ΔM_{L0} = amplitude of the Load Input Function

$\Omega_A = 2\pi f_A$ = excitations frequency

$\Psi_{2\alpha}$, $\Psi_{2\beta}$	α- and β- components of the rotor flux linkage
$i_{2\alpha}$, $i_{2\beta}$	α- and β-components of the rotor current
Zp	number of pole pairs.

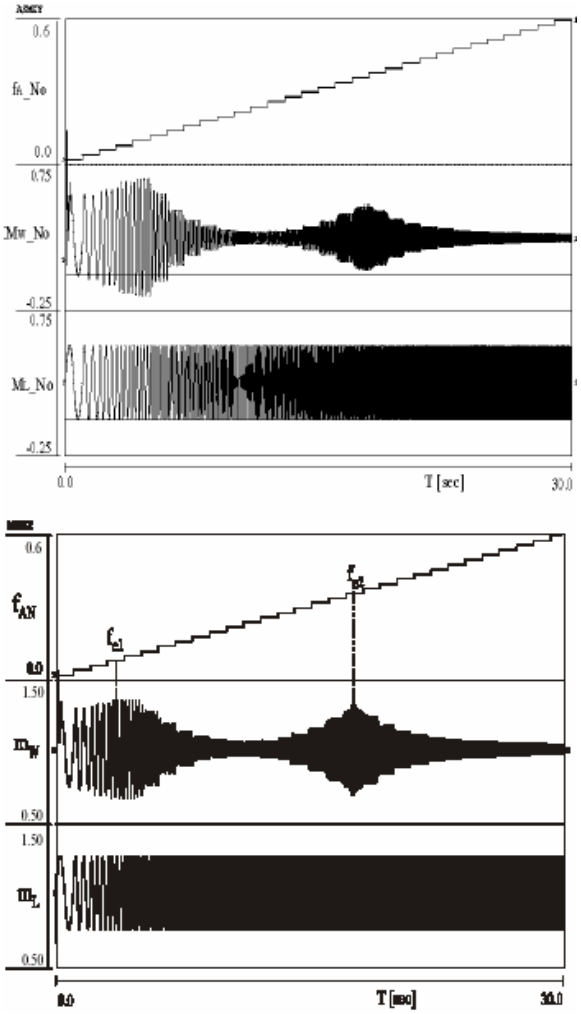

Fig.3 Normalised load-torque *ML_No,* shaft-torque *MW_No* and excitation frequency *fA_No*. Simulation *(top)* basic load ML0=25% and amplit. .ML0=25%. *(bottom)* basic load ML0=100%and ampl..ML0=25%.

This motor torque, which is estimated by relation (11), is transmitted to the mechanical part. The simulated curves (figure 3) have been digitally generated by the NETASIM- Software. On the Yaxis are represented the values of the load-torque, shaft-torque and excitation frequency related to the nominal values M_N=195 Nm respectively f_N=50 Hz. The time is shown on the X-axis.

1.3. Experiments of single cage IM

The simulation results have been validated with measurements at the test bench. The test bench from fig.1 is available at the Institute for Electrical Power Engineering at the Technical University of Clausthal in Germany *(Tulbure, 2003).*

For the first experiment this bench is composed of single cage induction machine, converter-fed DCmotor to generate the Load-Input-Function (LIF) and the flexible shaft between the masses. Some important parameters of this bench are contained in the table 1.

Table 1. Parameters of the first test bench

Parameter	Value
AC-Motor power, P_{NAC}	30 kW
Nominal speed, n_N	1470 min^{-1}
Nominal torque, M_N	195 Nm
DC-Motor power, P_{NDC}	30 kW
Motor inertia, J_1	0.35 kgm^2
Load inertia, J_2	0.83 kgm^2
Natural frequency of mechanical system, f_a	14.7 Hz
Shaft damping, b	6.3 Nms
Shaft stiffness, c	2100 Nm/rad

The reference values for the load were externally produced by the signal generator and given to the reversible dc-converter. This thyristor-converter feeds the excitation circuit of the dc-machine to generate in this way the LIF.

The shaft-torque *Mw* has been oscillographed in the XY Wave-Form in dependance on the excitation frequency *fA* (figure 4).

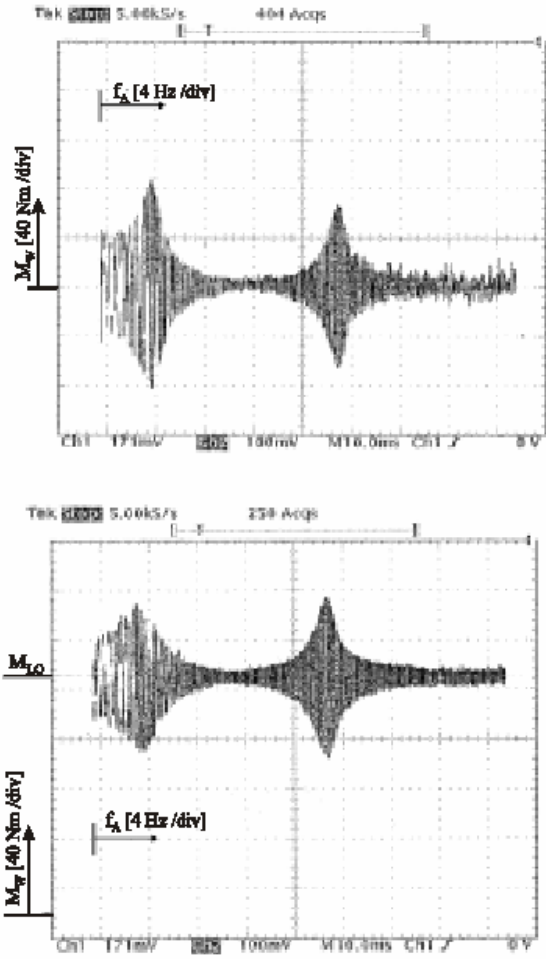

Fig.4 XY-Format of the shaft torque in dependence on the excitation frequency fA. Experimental results *(top)* basic load ML0=0% and amplitude .ML0=25% and *(bottom)* ML0=100% and amplit. .ML0=25%.

In fig. 4 the measurement results for the shaft torque in dependence on the stationary operating points are presented. The results show that the shaft torque magnitude is a function of the stationary operating point (slip) of the machine (Richter, 1983). Two resonance places are to be observed at about f_1=4 Hz and f_2=18 Hz (fig.4), respectively ω_1=25.1 1/s and ω_2=113.1 1/s in figure 2 (0 . s . 0.02).

2. SIMULATION AND VALIDATION OF THE DOUBLE CAGE INDUCTION MACHINE

In the second investigations step the frequency response of the transfer function G(p) shaft-torque / load-torque fluctuation for the double cage induction machine (Fig.5) has been simulated.

$$G(p) = \frac{\Delta M_W(p)}{\Delta M_L(p)} \qquad (13)$$

The results show that like in the first step, the shaft torque magnitude is a function of the stationary operating point (slip) of the machine. Slip is a motor property which depends on the rotor parameter.

For the mains operated machine with double cage, two resonance sites (simulation Fig.5 curve b) and measurement (Fig.6) at about f_1=4 Hz and f_2=17 Hz can be observed. The measurements (see the waveforms in Fig.6 top and bottom) confirm the afirmation, that the damping capacity is much higher for the induction machine with starting cage only.

The proposed combination to adjust the shaft oscillations is based on this statement, as more rotor resistance as little oscillations amplitude. This concept has been applied in the practice for the double-cage induction machine (DoCa-IM). In this case the variation of rotor parameters (R`L and X`L) is achieved by turn-on and -off between the cages with help of the Switching Device (DE) see Fig. 7

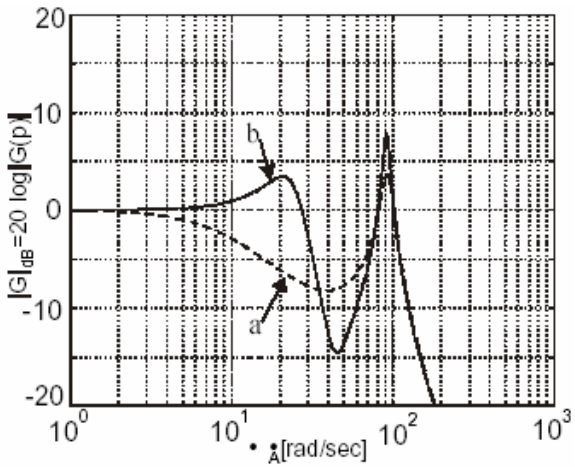

Fig.5 Bode-diagram of G(p) for the double cage IM a) with starting cage only b) with both cages.

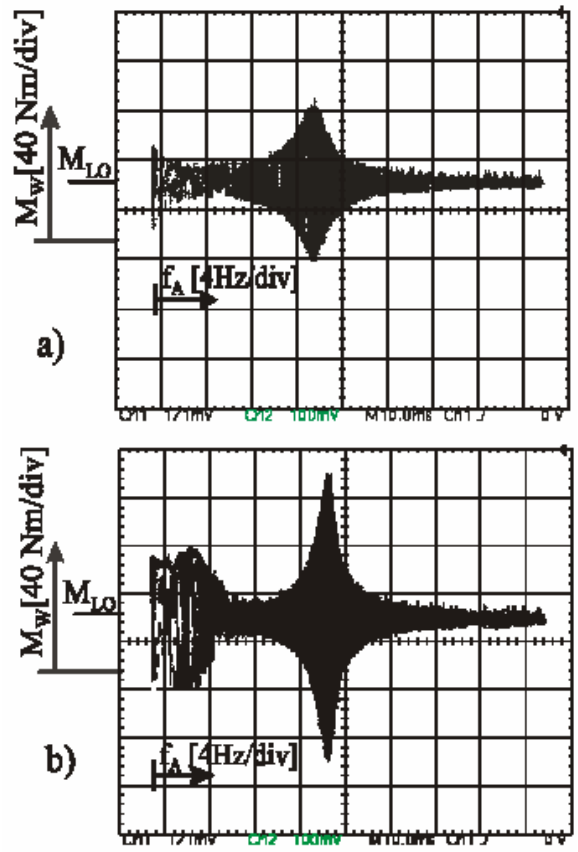

Fig.6 Measurement of the shaft-torque M_W as function of the excitation frequency f_A: a) IM with starting cage only; b) double cage IM.

3. DESIGN OF THE MACHINE WITH SWITCHING CAGES

3.1.Simulation in the time domain

By the new machine the secondary circuit from Fig. 7 is characterised by Ra, La common resistance and inductance for both cages, L_A, L_B and R_A, R_B starting cage and working cage inductance respectively reactance. The performance characteristics of the machine depend on the rotor current distribution in the starting or working cage (Leonhard,1997).

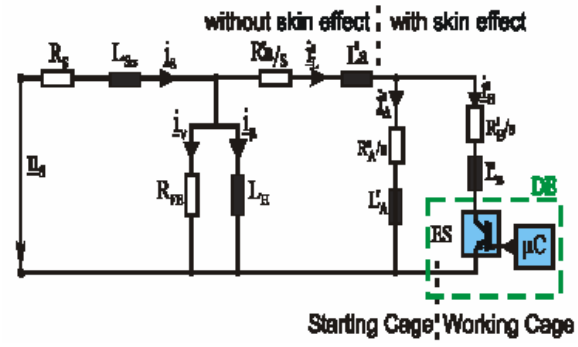

Fig.7 Equivalent electrical circuit of the DoCa-IM with switching device (DE).

Tab.2 Characteristic data of the double cage induction machine

Parameter	Symbol	Value	P.u.
Nominal slip	s_N	0.02	2
Breakdown slip	S_k	0.10	10
Stator resistance	Rs (Ω)	0.071	1.5
Starting cage resist.	R'_A (Ω)	0.670	14.3
Working cage resist.	R'_B (Ω)	0.330	7.2
Stator leakage reactance	$R_{S\sigma}$ (Ω)	0.192	4.2
Starting cage leakage reactance	x'_A (Ω)	0.177	3.8
Working cage leakage reactance	x'_B (Ω)	0.925	20.1
Rotor leakage without skin	x'_S (Ω)	0.050	1.1
Mutual reactance	X'_H (Ω)	11.80	256.6
Nominal impedance	Z_N (Ω)	4.60	100

In order to obtain good simulation results it is necessary to identify the electrical parameters of the model (Tab.2). The used mathematical model *(Leonhard, 1997)* of a machine consists of:

• equations of the electrical circuits, resp. stator and rotor windings (eq.14) and (15);

• equations of the electromagnetic field inside the machine (16, 17);

• equations of the mechanical motion of the rotor (11,12).

Will be selected the flux as state variable, the equations (14) and (15) can be rewrite:

$$\vec{u}_1 = r_1 \cdot \vec{i}_1 + T_N \cdot \frac{d\vec{\Psi}_1}{dt} + j \cdot \omega_K \cdot \vec{\Psi}_1 \qquad (14)$$

$$\vec{u}_2 = r_2 \cdot \vec{i}_2 + T_N \cdot \frac{d\vec{\Psi}_2}{dt} + j \cdot (\omega_K - \omega_{Le}) \cdot \vec{\Psi}_2 \qquad (15)$$

$$\vec{\Psi}_1 = x_1 \cdot \vec{i}_1 + x_h \cdot \vec{i}_2 \qquad (16)$$

$$\vec{\Psi}_2 = x_h \cdot \vec{i}_1 + x_2 \cdot \vec{i}_2 \qquad (17)$$

Will be selected the flux as state variable, the equations (14) and (15) can be rewrite:

$$T_N \frac{\mathrm{d}}{\mathrm{d}t} \cdot \begin{bmatrix} \dot{\vec{\Psi}}_1^k \\ \dot{\vec{\Psi}}_2^k \end{bmatrix} = \begin{bmatrix} c_{11} & c_{12} \\ c_{21} & c_{22} \end{bmatrix} \cdot \begin{bmatrix} \dot{\vec{\Psi}}_1^k \\ \dot{\vec{\Psi}}_2^k \end{bmatrix} + \begin{bmatrix} 1 & 0 \\ 0 & 1 \end{bmatrix} \cdot \begin{bmatrix} \vec{u}_1^k \\ \vec{u}_2^k \end{bmatrix} \qquad (18)$$

From the complex matricial equation (18) results the relation (19) with the notations (20)...(23):

$$\underline{I} \cdot T_N \cdot \dot{\underline{\psi}} = \underline{B} \cdot \underline{\psi} + \underline{I} \cdot \underline{u} \qquad (19)$$

$$\underline{\psi} = \begin{bmatrix} \psi_{1A} & \psi_{1B} & \psi_{2A} & \psi_{2B} \end{bmatrix}^T \qquad (20)$$

$$\underline{u} = \begin{bmatrix} u_{1A} & u_{1B} & u_{2A} & u_{2B} \end{bmatrix}^T \qquad (21)$$

$$\underline{I} = \begin{bmatrix} 1 & 0 & 0 & 0 \\ 0 & 1 & 0 & 0 \\ 0 & 0 & 1 & 0 \\ 0 & 0 & 0 & 1 \end{bmatrix} \qquad (22)$$

$$\underline{B} = \begin{bmatrix} b_{11} & b_{12} & b_{13} & b_{14} \\ b_{21} & b_{22} & b_{23} & b_{24} \\ b_{31} & b_{32} & b_{33} & b_{34} \\ b_{41} & b_{42} & b_{43} & b_{44} \end{bmatrix} = (b_{ij}) \qquad (23)$$

The elements of the matrices a_{ij}, b_{ij}, c_{ij} are calculated using the parameters from the Tab.2.

3.2. Practical realisation

The starting cage (top winding), being of higher resistance R_A and lower leakage inductance L_A, is placed below the rotor surface. In the working cage (bottom winding) in contrast, because the bars are located deep in the iron, the leakage inductance L_B is higher. Because of $R_A > R_B$ and $L_B > L_A$ the two cages are electrically complementary. The switching unit (DE) is composed of an electronically power switch (ES) and a microcontroller (μC). The ES is able to switch the working cage off and on and consists of a combination of multiphase rectifier with Schottky-diodes and an IGBT-breaker.

The necessary signals for the command of the semiconductor which is generated by the microcontroller, are sent from the stator to the rotor through a transmission system (Tulbure, 2003).

Fig.8 Three phase induction machine with cageswitching. (*top)* rotor with integrated power electronics *(bottom)* three phase stator.

4. EXPERIMENTS BY MACHINE WITH SWITCHING CAGES

4.1. Measurement infrastructure

The induction machine is connected directly to the three phase power supply network. With the help of a mettering shaft the signal corresponding to the torque values in the shaft (mw) is acquisited and processed. The load torque (mL) is generated through a dcmachine. The current and voltage are acquisited from stator side only for one phase, because the motor is considered as a symmetric consumer.

The switching signal on the gate of in rotor integrated transistors Upwm, is delivered on the one microcontroller port.

4.2. Comparison of the simulated and experimental results

In fig. 10 and 11 the results in time domain corresponding to the analyzed signals, load torque mL, shaft torque mW, phase current i1 and control signal Upwm are presented. In the case of simulation from fig.10 the results are normalised to the nominal values of torque and phase current.

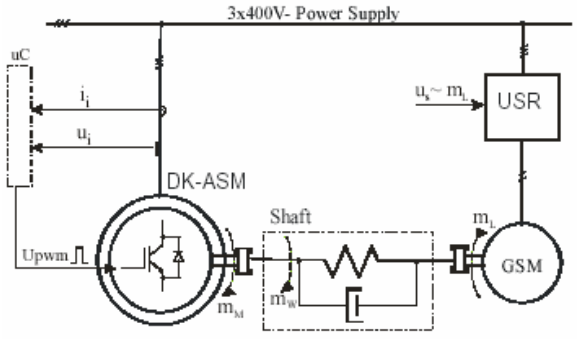

Fig.9 Preview of the measurements systems

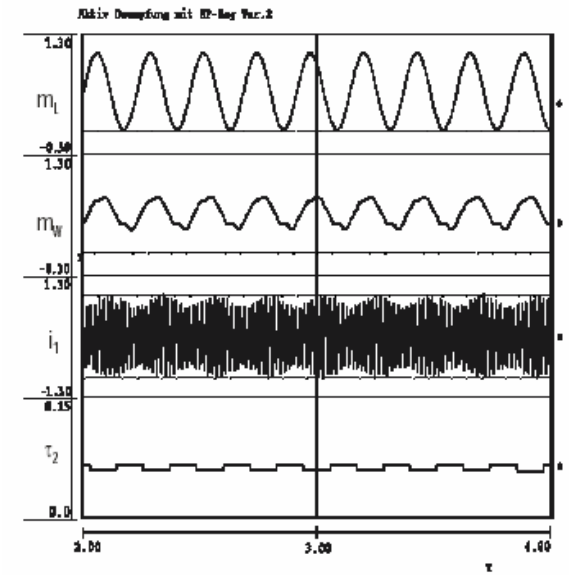

Fig. 10 Simulated waveform of load- m_L shaft-torque m_W, current i_1 and rotor time factor τ_2

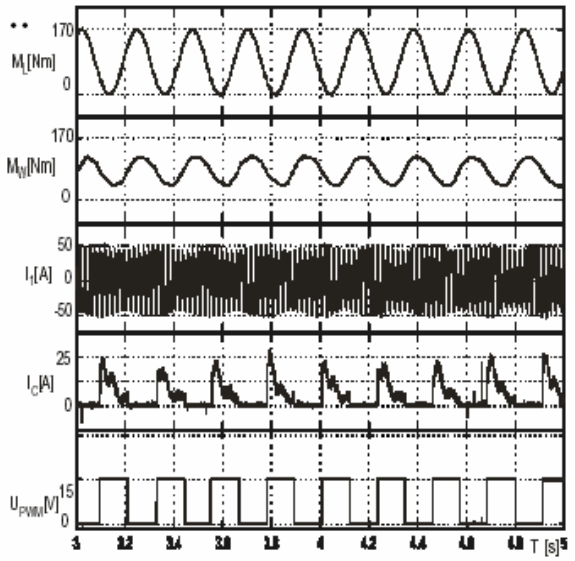

Fig.11 Measurements of load-torque m_L shaft-torque m_W, phase current i_1,collector current i_C and rotor time factor τ_2

The waveforms show a good corespondance of the simulation with the measurements. The switching task will be carried out by the semiconductor device mounted in the rotor of the machine. This switching unit make possible a dynamic and low-loss adjustment of the characteristic curve of the motor.

Comparisons of run tests have been demonstrated that the amplitude of the shaft torque oscillations can be adjusted by switching between starting and working cage of the machine.

REFERENCES

Beck, H.-P.; C. Sourkounis , A. Tulbure (2001), *Schwingungsdämpfung in Antriebssystemen mit Doppelkäfig-Asynchronmaschine.* VDI-Bericht **Nr. 1606**, pp. 113-126, Düsseldorf.

Leonhard, W. (1997), *Control of electrical drives*, pp. 178-192, 240-265, Ed.Springer. Berlin

MATLAB 7.1. (2005), *User Manual*, The MathWork Inc., USA 2005

NETASIM 2.5 (1992), Benutzerhandbuch, Daimler-Benz AG, Berlin 1992

Richter, K. (1983), *Verhalten von Antriebssystemen mit Asynchronmotoren bei erzwungenen Schwingungen,* Freiberger F-Hefte, pp. 63-71, Leipzig.

Schröder, D. (2001), *Elektrische Antriebe. Regelung von Antriebssystemen*, pp.420-434,804-810, Ed.Springer, Heidelberg.

Tulbure, A. (2003), *Netzgespeiste Asynchronmaschine mit elektronischer Käfigumschaltung zur aktiven Schwingungsbedämpfung*. Doctoral Thesis, Univ. of Technology Clausthal, Germany